

1    **Original article**

2

3    **Genetic factors outside the metabolic cluster for plastid-derived sesquiterpenes are required**  
4    **to pursue arthropod-resistant tomatoes**

5    Rodrigo Therezan<sup>1,2</sup>, Ruy Kortbeek<sup>2</sup>, Eloisa Vendemiatti<sup>1</sup>, Saioa Legarrea<sup>3</sup>, Severino M. de Alencar<sup>4</sup>,  
6    Robert Schuurink<sup>2</sup>, Petra Bleeker<sup>2\*</sup>, Lázaro E. P. Peres<sup>1\*</sup>.

7

8    <sup>1</sup>Laboratory of Plant Developmental Genetics. Department of Biological Sciences, "Luiz de Queiroz"  
9    College of Agriculture, University of São Paulo, 13418-900, Piracicaba, SP, Brazil.

10    <sup>2</sup>Green Life Science Research Cluster, Swammerdam Institute for Life Sciences, University of  
11    Amsterdam, Science Park 904, 1098 XH Amsterdam, The Netherlands.

12    <sup>3</sup>Molecular & Chemical Ecology, Institute for Biodiversity and Ecosystem Dynamics, University of  
13    Amsterdam, PO Box 94240,1090 GE Amsterdam, The Netherlands.

14    <sup>4</sup>Department of Agri-Food Industry, Food and Nutrition, "Luiz de Queiroz" College of Agriculture,  
15    University of São Paulo, 13418-900, Piracicaba, SP, Brazil.

17

18    **\*Corresponding authors:**

19    Lázaro Estáquio Pereira Peres  
20    lazaro.peres@usp.br  
21    Escola Superior de Agricultura "Luiz de Queiroz"  
22    University of São Paulo - USP  
23    Av. Padua Dias, 11 CP. 09  
24    13418-900 Piracicaba - SP  
25    BRAZIL

26  
27    Petra Bleeker  
28    P.M.Bleeker@uva.nl  
29    Swammerdam Institute for Life Sciences  
30    University of Amsterdam  
31    Dept. Plant Physiology  
32    Science Park 904, room C2.213  
33    1098 XH Amsterdam  
34    THE NETHERLANDS

35

36    **One-sentence summary:** Cultivated tomatoes harboring the plastid-derived sesquiterpenes from *S. habrochaites* need additional genetic components necessary to convert them into effective  
37    insecticides.  
38

39

40

41 **Author contributions:**

42 L.E.P.P. and P.B. planned and designed the research; L.E.P.P. designed the introgression.  
43 R.T., R.K., E.V. and S.L.I. performed experiments and helped to analyze data; S.M.A. and R.S.  
44 helped to analyze data. R.T., L.E.P.P. and P.B. wrote the manuscript. All authors read and approved  
45 the final manuscript.

46 **Conflict of Interest:**

47 The authors have no conflicts of interest to declare.

48

49 **Funding information:**

50 This work was supported by CAPES-Brazil, CNPq-Brazil, and FAPESP-Brazil. E.V. and  
51 L.E.P.P. received scholarship (2016/22323-4) and grant (2018/05003-1) from FAPESP. R.T. received  
52 scholarship from CAPES (88881.189015/2018-01). SMA and LEPP received fellowships from CNPq  
53 (grants 307893/2016-2 and 306518/2018-0, respectively). RK was supported through the Netherlands  
54 Science Foundation (NWO) research incentive TTI-Vidi (project 12988).

55

56

57

58

59

60

61

62

63

64

65

66

67

68

69

70

71 **ABSTRACT**

72 To deal with arthropod pests the tomato wild relatives produce a variety of defense  
73 compounds in their glandular trichomes. In *Solanum habrochaites* LA1777, a functional cluster of  
74 genes on chromosome 8 controls plastid-derived sesquiterpene synthesis not found in cultivated  
75 tomatoes. The main genes at the cluster are *Z-prenyltransferase* (*zFPS*) that produces Z-Z-farnesyl  
76 diphosphate (Z,Z-FPP), and *Santalene and Bergamotene Synthase* (*SBS*) that uses Z,Z-FPP to produce  
77 α-santalene, β-bergamotene, and α-bergamotene in type-VI glandular trichomes. Both LA1777 and  
78 cultivated tomatoes have type-VI trichomes, but the gland in cultivated tomato is much smaller  
79 containing low levels of monoterpenes and cytosolic-derived sesquiterpenes, which do not provide  
80 tomato with the same pest resistance as in LA1777. We successfully transferred the plastid-derived  
81 sesquiterpene pathway from LA1777 to type-VI trichomes of a cultivated tomato (cv. Micro-Tom,  
82 MT) by a back-crossing approach. The trichomes of the introgressed line named MT-*Sesquiterpene*  
83 *synthase 2* (MT-*Sst2*) produced even higher levels of α-santalene, β-bergamotene, and α-bergamotene  
84 than the type-VI glandular trichomes of LA1777. We also noticed that the type-VI trichome internal  
85 storage-cavity size increases in MT-*Sst2*, probably as an “inflated balloon” effect of the increased  
86 amount of sesquiterpenes. Surprisingly, the presence of high amounts of plastid-derived  
87 sesquiterpenes was not sufficient to confer resistance to various tomato pests in MT-*Sst2*. Since MT-  
88 *Sst2* made the same sesquiterpenes as LA1777, this points to additional factors, outside the genomic  
89 region thought to be the metabolic cluster, necessary to obtain arthropod-resistant tomatoes. Our  
90 results also provide a better understanding of the morphology of *S. habrochaites* type-VI trichomes.  
91

92

93 **Keywords:** Type-VI trichomes, tomato trichomes, santalene, bergamotene, *Solanum habrochaites*,  
glandular trichome.

94

95

96 **INTRODUCTION**

97 Isoprenoids are the most abundant and diverse class of compounds produced by plants with  
98 a wide variety of biological functions (Dudareva *et al.*, 2013). They are produced through combining  
99 multiple five-carbon units (C5) of isoprene and are essential for plant growth and development. They  
100 participate as precursors for several components of essential processes like photosynthesis,  
101 respiration, cell cycle control (Estévez *et al.*, 2001) and plant hormones such as gibberellins, abscisic  
102 acid, brassinosteroids and strigolactones (Falara *et al.*, 2011). Isoprenoids also play an important role

103 in the interactions of plants with the environment, including defense against herbivorous insects and  
104 attraction of pollinators (Dudareva *et al.*, 2013).

105 In plants, all isoprenoids originate from two distinct metabolic pathways: the mevalonate  
106 (MVA) pathway, located in the cytosol and the 2-C-methyl-D-erythritol 4-phosphate (MEP) pathway  
107 located in plastids. Both pathways produce isopentenyl diphosphate (IPP) and dimethylallyl  
108 diphosphate (DMAPP), the isoprene building blocks used by terpene synthases (TPSs) to catalyze  
109 the formation of C10 monoterpenes, C15 sesquiterpenes or C20 diterpenes (Tholl, 2006).

110 In cultivated tomato (*Solanum lycopersicum*), sesquiterpene biosynthesis usually takes place  
111 in the cytosol from the MVA pathway. However, in glandular trichomes of the wild tomato species  
112 *S. habrochaites*, sesquiterpenes are also produced in the plastids from the MEP pathway (Sallaud *et*  
113 *al.*, 2009). The presence of plastid-derived sesquiterpenes in some wild species has been described to  
114 be responsible for the decreased damage by insects, making these wild species naturally resistant to  
115 multiple pests such as lepidopterans (Eigenbrode *et al.*, 1994; Eigenbrode *et al.*, 1996), whiteflies  
116 (*Bemisia spp.*) (Bleeker *et al.*, 2012) and also spider mites (Maluf *et al.*, 2001).

117 Two independent loci have been associated with the biosynthesis of two different classes of  
118 sesquiterpenes in *S. habrochaites*. The *Sesquiterpene synthase 1* (*SsT1*) locus on chromosome 6 is  
119 responsible for the accumulation of cytosol-derived sesquiterpenes. At this locus, *TPS12* is associated  
120 with  $\beta$ -caryophyllene and  $\alpha$ -humulene biosynthesis and *TPS9* with the production of germacrenes.  
121 The *S. habrochaites* *TPS9* allele (*ShTPS9*) is associated with germacrene B and D production  
122 (Hoeven van der *et al.*, 2000; Bleeker, Spyropoulou, *et al.*, 2011; Falara *et al.*, 2011). The existence  
123 of *SlTPS9*, that makes germacrene C, was also reported for the cultivar VFNT Cherry (Colby *et al.*,  
124 1998), but it is worth noting that this cultivar has introgressions of the wild species *S. peruvianum* on  
125 chromosome 6. The second locus harboring sesquiterpenes synthases is the *Sesquiterpene synthase 2*  
126 (*SsT2*) locus on chromosome 8. At this locus *S. habrochaites* has a cluster of TPSs (*TPS18*, *TPS20*  
127 and *TPS45*) encoding enzymes responsible for the accumulation of plastid-derived sesquiterpenes,  
128 including  $\alpha$ -santalene,  $\alpha$ -bergamotene,  $\beta$ -bergamotene and 7-epizingiberene (Sallaud *et al.*, 2009;  
129 Bleeker, Diergaarde, *et al.*, 2011). In cultivated tomato, a cluster of five functional TPS genes  
130 (*TPS18*, *TPS19*, *TPS20*, *TPS21*, and *TPS41*) is present in the equivalent locus on chromosome 8  
131 (Falara *et al.*, 2011). In addition, this same chromosomal region also contains the *Neryl Diphosphate*  
132 *Synthase 1* (*SlNDPS1*) gene, which codes for an enzyme catalyzing the formation of neryl  
133 diphosphate (NPP). NPP is used by tomato *TPS20* to synthesize  $\beta$ -phellandrene and several other  
134 monoterpenes in the plastids (Falara *et al.*, 2011; Matsuba *et al.*, 2013). In *S. habrochaites* the *cis*-  
135 *Farnesyl Diphosphate Synthase* (*zFPS*) gene is homologous to the *SlNDPS1* gene (Matsuba *et al.*,  
136 2013). The *zFPS* codes for a Z-prenyltransferase that catalyzes the synthesis of Z-Z-farnesyl  
137 diphosphate (Z,Z-FPP) from IPP and DMAPP. The *TPS45* gene from *S. habrochaites* LA1777

138 encodes a *Santalene and Bergamotene Synthase (SBS)* that uses *Z,Z*-FPP as a substrate to produce  
139 plastid-derived sesquiterpenes (Sallaud *et al.*, 2009; Matsuba *et al.*, 2013). Both *zFPS* and *SBS*  
140 contain putative chloroplast targeting sequences allowing the biosynthesis of the sesquiterpenes in  
141 this organelle.

142 The *zFPS* and *SBS* genes are specifically expressed in type-VI glandular trichomes (Sallaud  
143 *et al.*, 2009) that harbor chloroplasts and are present on several tomato wild-relatives (Kang *et al.*,  
144 2010; Glas *et al.*, 2012; Balcke *et al.*, 2017). In cultivated tomato, type-VI trichomes contain a single  
145 basal cell connected to a short (~0.1 mm) unicellular stalk which is connected by an intermediate cell  
146 to the four-celled glandular head containing chloroplasts and other organelles (Bergau *et al.*, 2015).  
147 In *S. habrochaites*, the stalk is longer (~0.2 mm) and the trichome has a round glandular head instead  
148 of visible 4 distinct cells (Besser *et al.*, 2009).

149 In general, cultivated tomatoes are highly vulnerable to several arthropod pests, which  
150 include whiteflies, spider mites, and thrips. In addition, some pest, such as whiteflies can spread  
151 viruses (Moodley *et al.*, 2019). Under heavy infestation, these pests can cause a reduction of plant  
152 vigor and yield which can lead to huge losses in productivity (Wakil *et al.*, 2018). Consequently, to  
153 minimize the damage caused by pests, high amounts of pesticides have been applied in agri- and  
154 horticulture (Silva *et al.*, 2011). In this sense, an alternative to chemical pest control could be the use  
155 of commercial tomatoes carrying favorable genetic factors from tomato wild species. Herein, we  
156 investigated whether the introduction of the genetic pathway for plastid-derived sesquiterpenes from  
157 a wild species into cultivated tomato could increase resistance to arthropod tomato pests. We show  
158 that the *Sst2* gene cluster that controls santalene and bergamotene production in *S. habrochaites*  
159 LA1777 can be effectively transferred to cultivated tomato (cv. Micro-Tom) and function in its type-  
160 VI trichomes. Tomato type-VI trichomes that accumulated high levels of plastid-derived  
161 sesquiterpenes also increased the size of the internal gland cavity, providing a better understanding  
162 of differential trichome morphology. We further demonstrated that, the high production of “wild  
163 tomato sesquiterpenes” was not sufficient to confer resistance to tomato-pests. Apparently genetic  
164 factors outside the metabolic cluster on chromosome 8 are required for the production of the anti-  
165 insect compounds in *S. habrochaites*.

166

## 167 RESULTS

### 168 **Introgression of *Sst2* gene cluster from *S. habrochaites* LA1777 into *S. lycopersicum* cv. 169 Micro-Tom (MT)**

170 In order to introduce the plastid-derived sesquiterpene pathway into the Micro-Tom (MT)  
171 cultivar, we crossed *S. habrochaites* LA1777 with a MT line harbouring the *lutescent 1* mutation

172 (MT-*l1*) and used it as a recurrent parent (Fig.1A). Both the *lutescent 1* mutation and the *SsT2* locus  
173 map at the short arm of the chromosome 8 (Tanksley *et al.*, 1992; Sallaud *et al.*, 2009). The *lutescent*  
174 *1* phenotype comprises a premature and progressive yellowing of the leaves due to impaired  
175 chlorophyll accumulation (starting from the base of the plant) (Fig S1 A and B), a lack of chlorophyll  
176 accumulation in the pistils (Fig S1 C) and whitish-yellow fruits (Barry *et al.*, 2012). This allowed us  
177 to introgress the *S. habrochaites* *SsT2* locus into MT by a relatively easy visual selection of the  
178 progeny. In each generation of introgression, we selected for plants not presenting the *lutescent 1*  
179 phenotype, which implies the presence of the equivalent chromosome segment of *S. habrochaites*  
180 containing the *SsT2* locus. In the F<sub>2</sub> generation, plants not harbouring the *lutescent 1* mutation were  
181 used for back-crossing (BC) with MT-*l1*. This procedure was repeated in the BC<sub>1</sub> and subsequent  
182 generations. After six BC generations and self-pollination (BC<sub>6</sub>F<sub>2</sub>) using the visual marker, we  
183 employed CAPS markers based on single nucleotide polymorphisms (SNPs) for a genetic screen for  
184 homozygous plants harbouring the *SsT2* locus from the wild species. In the BC<sub>6</sub>F<sub>3</sub> generation and  
185 generations thereafter (BC<sub>6</sub>F<sub>n</sub>), the obtained plants were considered a near isogenic line (NIL), no  
186 longer segregating for the presence of the wild sesquiterpenes pathway and other traits. The NIL was  
187 named MT-*Sesquiterpene synthase 2* (MT-*Sst2*).

188 We employed CAPS markers to determine the size of the fragment introgressed into the  
189 MT background. Genetic mapping positioned the introgressed region between *Solyc08g005020* and  
190 *Solyc08g007130* on the top of chromosome 8 (Fig. 1B). The introgressed region overlaps with the  
191 mapping position of *SsT2* previously reported by Sallaud *et al.* (2009), which also confirmed that  
192 both *zFPS* and *SBS* genes were mapped to this region. The introgressed region in MT-*Sst2* is  
193 furthermore consistent with the *SsT2* locus found in a set of ILs between *S. lycopersicum* × *S.*  
194 *habrochaites* LA1777 that were able to produce plastid-derived sesquiterpenes (Hoeven van der *et*  
195 *al.*, 2000).

196 Additionally, we analysed the relative transcript levels of *zFPS* and *SBS* by quantitative RT-  
197 PCR in trichomes of MT-*Sst2* and *S. habrochaites* LA1777. Both genes were indeed expressed in  
198 MT-*Sst2* but transcripts levels were significantly lower in MT-*Sst2* compared to the wild parent (Fig.  
199 2).

200 **Production of the sesquiterpenes santalene and bergamotene in the Micro-Tom line harboring  
201 the *S. habrochaites* *SsT2* locus**

202 To confirm the presence of the *S. habrochaites* sesquiterpene pathway in the MT-*Sst2* line,  
203 we performed Gas-chromatography Mass-Spectrometry (GC-MS) analyses on isolated type-VI  
204 trichome glands. The type-VI trichomes of the MT-*Sst2* line not only accumulated sesquiterpenes,

205 but also produced higher amounts of these plastid-derived sesquiterpenes, compared to parental *S.*  
206 *habrochaites* LA1777 (Fig. 3).

207 As expected, we did not detect the monoterpenes found in the MT parental in the MT-*Sst2*  
208 line (Fig. 3, (peaks 1, 2 and 3), Fig S2). Since the monoterpenes 2-carene,  $\alpha$ -phellandrene and  $\beta$ -  
209 phellandrene and D-limonene are produced by enzymes encoded by *SITPS20* genes on tomato  
210 chromosome 8, it was predicted that these monoterpenes on homozygous MT-*Sst2* plants would be  
211 replaced by the sesquiterpenes produced by enzymes encoded by the wild species alleles on the same  
212 chromosomal region. Indeed, the MT-*Sst2* line produced the plastid-derived sesquiterpenes ( $\alpha$ -  
213 bergamotene,  $\alpha$ -santalene, exo- $\alpha$ -bergamotene, epi- $\beta$ -santalene, and endo- $\beta$ -bergamotene), also  
214 present in *S. habrochaites* LA1777 (Fig. 3A and B). Although we found high levels of plastid-derived  
215 sesquiterpenes in the MT-*Sst2* line, we did not detect any carboxylic acid derivatives from santalene  
216 or bergamotene, as in the wild species (Fig. 3A, peaks 14, 15 and 16, and 3C). As expected, no  
217 santalene or bergamotene was present in control MT trichomes (Fig. 3A, C and S2). However, not  
218 only was there a 7-fold increase in the plastid-derived sesquiterpenes of individual type-VI trichomes  
219 of MT-*Sst2* compared to LA1777, but it appeared that the MT-*Sst2* type-VI trichomes also produce  
220 substantially (2-fold) more cytosolic-sesquiterpenes when compared to MT (Fig. 3C).

221 **Production of mono and sesquiterpenes in type-VI trichomes under different allelic dosages**  
222 **at the *Sst2* locus**

223 In order to investigate how the allelic dosage at the *Sst2* locus affects the levels of mono  
224 and sesquiterpenes in type-VI trichomes, we selected homozygous *sst2/sst2* and *Sst2/Sst2*, and  
225 heterozygous *sst2/Sst2* MT plants. The molecular markers used for selection were designed based  
226 on polymorphisms found in the genomic sequence of cultivated tomato and LA1777 (Table S1).  
227 Note that there is no complete synteny between the *Sst2* locus of *S. lycopersicum*, and *S.*  
228 *habrochaites*. Hence, at this locus, *S. lycopersicum* contains the functional genes  
229 *TPS18*, *TPS19*, *TPS20*, *TPS21*, *TPS41* and *SINDPS1*, whereas *S. habrochaites* contains the  
230 functional genes *TPS18*, *TPS20*, *TPS45* (SBS) and *zFPS* (Matsuba *et al.*, 2013). Thus, the *sst2/Sst2*  
231 plants can be better considered hemizygous for both set of genes from each parental.

232 The amount of the monoterpenes did not differ significantly between homozygous *sst2/sst2*  
233 and hemizygous *sst2/Sst2* plants. As predicted, monoterpenes were absent in homozygous *Sst2/Sst2*  
234 plants (Fig. 4) since *SINDPS1* and *SITPS20* are not present in *Sst2/Sst2* plants. On the other hand,  
235 there was no significant effect of gene dosage for *SINDPS1* when comparing monoterpene content  
236 of homozygous *sst2/sst2* and hemizygous *sst2/Sst2* plants. Regarding the concentration of  
237 cytosolic-derived sesquiterpenes  $\beta$ -caryophyllene and  $\alpha$ -humulene, the hemizygous *sst2/Sst2* plants

238 did not differ significantly from homozygous *sst2/sst2* plants, while the homozygous *Sst2/Sst2* did,  
239 produced higher amounts of these compounds, especially  $\alpha$ -humulene (Fig.4).

240 The concentrations of all plastid-derived sesquiterpenes  $\alpha$ -bergamotene,  $\alpha$ -santalene, exo- $\alpha$ -  
241 bergamotene, epi- $\beta$ -santalene, and endo- $\beta$ -bergamotene were higher in the homozygous *Sst2/Sst2*  
242 type-VI trichomes when compared to the trichomes of hemizygous *sst2/Sst2* plants, indicating that  
243 these compounds are under the effect of gene dosage.

244 **Trichome abundance, morphology and gene expression in the Micro-Tom line harboring the *S.***  
245 ***habrochaites* genes in the *SsT2* locus**

246 We next verified if the locus substitution caused changes in abundance of different trichome  
247 types and the morphology of type-VI trichomes in adult leaves of the MT-*Sst2* line. The densities of  
248 type-VI trichomes were not altered in MT-*Sst2* compared to MT for both adaxial or abaxial leaf  
249 surfaces (Fig. 5A and 5B). The wild species showed significantly higher numbers of type-VI trichome  
250 on the adaxial and fewer numbers on the abaxial leaf surface (Fig. 5B).

251 We also observed that *S. habrochaites* LA1777 has a high density of type-IV trichomes (Fig.  
252 5B). Type-IV trichomes were previously associated with increased production of acylsugars  
253 providing resistance to insect pests in wild species (Simmons and Gurr, 2005). Type-IV trichome are  
254 however absent on adult leaves of MT and MT-*Sst2*, indicating that the introgressed segment on  
255 chromosome 8 from *S. habrochaites* LA1777 is not involved in controlling the presence of this type  
256 of trichomes. Type-V is the most abundant non-glandular trichome found on MT and MT-*Sst2*.  
257 Interestingly, we found an increased number of (non-glandular) type-V trichomes on both leaf  
258 surfaces in MT-*Sst2*. Approximately 2-fold more type-V trichomes were observed on the adaxial leaf  
259 surface of MT-*Sst2* compared with MT background (Fig. 5B).

260 The majority of glandular trichomes found in MT and MT-*Sst2* was type-VI. We next  
261 analysed the gland and internal cavity size of the type-VI glandular trichomes (Fig. 5A and C). There  
262 is no significant difference between the MT and MT-*Sst2* gland size. However, the size of the internal  
263 cavity is increased in MT-*Sst2* compared to MT. The introgression line also appears to exhibit a  
264 (subtle but significant) increase in stalk length compared to MT, but still the stalk is much shorter  
265 than that of type-VI trichomes found in LA1777 (Fig. 5A and C).

266 **Herbivore resistance of the Micro-Tom line with increased amounts of santalene and**  
267 **bergamotene**

268 In order to verify if the increase in plastid-derived sesquiterpenes in type-VI trichomes of  
269 MT-*Sst2* would result in improved resistance to herbivores, we conducted no-choice bioassays using

270 four relevant pests in tomato. In the whitefly bioassay, survival of whiteflies did not differ between  
271 MT-*Sst2* and MT plants, while the LA1777 displayed a high reduction in the survival of this pest.  
272 Almost 80% of the whiteflies survived on MT-*Sst2*, whereas less than 40% survived on the wild  
273 tomato species (Fig. 6A).

274 Next, bioassays using the defense-suppressing spider mite *Tetranychus evansi* and the  
275 defense-inducing spider mite *Tetranychus urticae* were performed. Both MT and MT-*Sst2* showed  
276 100% of both spider mites surviving, while on *S. habrochaites* LA1777 only approximately  
277 20% of *T. evansi* and 40% of *T. urticae* survived after 2 days (Fig. 6B). Oviposition rates of both  
278 spider mite species were equal on MT-*Sst2* and MT leaf disc, as they were strongly reduced in the  
279 wild species (Fig. 6C).

280 Finally, we conducted a bioassay with the western flower thrips (*Frankliniella occidentalis*)  
281 comparing adult survival on MT, MT-*Sst2* and the wild species. Again, there were no significant  
282 differences in survival or egg hatching observed as a result of the *Sst2* introgression (Fig. 6D and E).  
283 Female thrips were still able to oviposit in both genotypes and the larvae hatched from the eggs  
284 reaching the larval stage. Conversely, significant reductions in the number of surviving adults and  
285 the number of emerged larvae were observed for the wild species.

## 286 DISCUSSION

### 287 ***Solanum habrochaites* plastid-derived sesquiterpene synthesis can be transferred to type-VI 288 trichomes of cultivated tomato.**

289 We successfully introgressed the *SsT2* gene cluster responsible for the biosynthesis of  
290 plastid-derived sesquiterpene pathway from *S. habrochaites* LA1777 into the genetic model system  
291 cv. Micro-Tom (MT) (Fig 1A). The genes transferred were expressed into the tomato type-VI  
292 trichomes (Fig. 2) and resulted in the production of high levels of plastid-derived sesquiterpenes (Fig.  
293 3C).

294 The allelic dosage influenced the plastid-derived sesquiterpenes levels produced in type-VI  
295 trichomes. The levels of all plastid-derived sesquiterpenes were higher in the homozygous *Sst2/Sst2*  
296 plants than the hemizygous *sst2/Sst2* (Fig.4). This can be explained by the presence of just one copy  
297 of both *zFPS* and *SBS* alleles in hemizygous *sst2/Sst2* plants. It can also be the result of the presence  
298 of both *SINDPS1* and *zFPS* in the hemizygous *sst2/Sst2* acting in the same compartments (plastids)  
299 and competing for a limited amount of IPP and DMAPP in type-VI trichomes (Dudareva *et al.*, 2005;  
300 Besser *et al.*, 2009; Schilmiller *et al.*, 2009). However, it is unlikely that plastid-derived monoterpene  
301 production can limit the substrate for the production of sesquiterpenes in plastids, since the levels of

302 monoterpenes are much lower than the plastid-derived sesquiterpenes (Fig. S2, Fig. 4) (Banerjee *et* al., 2013). In addition, due to differences in substrate affinity, zFPS would use the IPP or DMAPP to  
303 produce Z,Z-FPP more efficiently than SINDPS1 uses to produce NPP in the plastids (Sallaud *et al.*,  
304 2009; Kang *et al.*, 2014).

306 Despite the fact that the introgression line MT-Sst2 produced significantly higher levels of  
307 santalene and bergamotene in type-VI glands compared to LA1777 (Fig 3), we did not detect  
308 sesquiterpene derivatives in MT-Sst2 as they are present in the wild species (Fig.3A and C). The  
309 absence of  $\alpha$ -santalenoic and  $\alpha$ - and  $\beta$ -bergamotenoic acids in the MT-Sst2 line likely explains the  
310 higher levels of santalene and bergamotene, compared to the wild species. In *S. habrochaites*  
311 LA1777, santalene and bergamotene are converted to derivatives identified as sesquiterpene  
312 carboxylic acids,  $\alpha$ -santalenoic, and  $\alpha$ - and  $\beta$ -bergamotenoic acids (Coates *et al.*, 1988). Notably,  
313 high sesquiterpene levels in MT-Sst2 compared to LA1777 provide an indirect evidence that  
314 santalene and bergamotene are used as precursors for further metabolism into corresponding alcohol  
315 and acids derivatives in LA1777 (Frelichowski and Juvik, 2005; Besser *et al.*, 2009; Gonzales-Vigil  
316 *et al.*, 2012).

317 The relative transcript levels of *zFPS* and *SBS* were higher in LA1777 compared to the  
318 introgressed line (Fig. 2). Since MT-Sst2 and LA1777 share the same chromosomal segment  
319 comprising the *SsT2* locus, it was expected that they have the same *cis*-regulatory elements  
320 controlling the expression of the *zFPS* and *SBS* genes. The lower expression of these genes in MT-  
321 Sst2 may suggest the involvement of a set of yet unknown trans-regulatory elements (e.g.  
322 transcription factors and other regulatory elements in different chromosomal regions) necessary to  
323 increase the expression of the genes present in the *SsT2* locus. Therefore, our results point at a role  
324 for additional genetic components that have not been introgressed. It has been shown that poor terpene  
325 producing genotypes have also drastically reduced transcript levels for key steps in the terpene  
326 biosynthesis pathway (Tissier, 2012), suggesting that the transfer of additional components enhancing  
327 *zFPS* and *SBS* expression could increase the content of sesquiterpenes in MT-Sst2 even further. Up  
328 to now, only a few transcription factors were proven to be involved in the regulation of terpene  
329 pathways in tomato (Spyropoulou *et al.*, 2014; J., Xu *et al.*, 2018), though these were not implicated  
330 as positive regulators of *zFPS* or *SBS* specifically.

331 We also noted that the concentration of the cytosolic-derived sesquiterpene  $\alpha$ -humulene was  
332 higher in homozygous *Sst2/Sst2* plants when compared to homozygous *sst2/sst2* and hemizygous  
333 *sst2/Sst2* plants. The TPS12 responsible for the production of  $\beta$ -caryophyllene and  $\alpha$ -humulene is  
334 encoded by a gene in the *SsT1* locus on chromosome 6, which is clearly outside of the region  
335 introgressed. Therefore, the *TPS12* in the *SsT1* locus is likely to have the same alleles for the three

336 genotypes and it could not be the cause of the high amount of  $\alpha$ -humulene in the homozygous  
337 *Sst2/Sst2* plants. Since  $\alpha$ -humulene coelutes with  $\beta$ -bergamotene (Hoeven van der *et al.*, 2000), we  
338 cannot exclude the possibility that the level of  $\alpha$ -humulene in MT-*Sst2* is overestimated.

339 **Introgression of *Sst2* appears to affect type-VI trichome morphology**

340 The MT-*Sst2* line with augmented contents of sesquiterpenes in type-VI trichomes displayed  
341 an increased glandular cavity volume (Fig 5C). A possible explanation for this is that the boost in the  
342 total amount of terpenes could result in a physical pressure in the cavity wall, forcing the internal  
343 cavity to inflate like a balloon, as similarly suggested by Ben-Israel *et al.*, (2009). However, the subtle  
344 increase in the internal cavity of MT-*Sst2* was not paired with an altered external gland shape.  
345 Modification in external gland shape depends both on genes related to cell wall remodelling  
346 (Bennewitz *et al.*, 2018) and on synthesis and accumulation of very high levels of compounds into  
347 the gland. Thus, a combination of genes controlling the high flux of metabolites with genes  
348 controlling the cell wall remodeling might push the gland to expand, creating the characteristic round  
349 type-VI trichome of *S. habrochaites*.

350 Stalk length is one of the morphologic characteristics used to identify the different types of  
351 trichomes in *Solanum* (Simmons and Gurr, 2005). The slightly increased type-VI trichome stalk  
352 length observed in MT-*Sst2* (Fig. 5C) is unlikely the result of the effect of the biosynthetic enzymes  
353 encoded on the *Sst2* locus. Recently Xu *et al.*, (2018c), demonstrated that the downregulation of  
354 *SlMYC1*, a bHLH transcript factor, results in plants with shorter type-VI trichome stalks. Since  
355 *SlMYC1* (*Slc08g005050*) is also located on top of chromosome 8, we specifically searched for this  
356 transcript factor in our introgressed line. Hence, the presence of the wild *ShMYC1* allele inside the  
357 region introgressed was confirmed by CAPS marks (Fig 1B and S3). In general, *S. habrochaites*  
358 species exhibit a longer type-VI trichome stalk compared to cultivated tomatoes (Simmons and Gurr,  
359 2005; Bergau *et al.*, 2015). The biological role for a higher stalk, or a taller trichome in the wild  
360 species is not described, but it is tempting to speculate that though the effect is marginal, the altered  
361 stalk length could be the result of replacement of *SlMYC1* with *ShMYC1*.

362 Furthermore, MT-*Sst2* displayed an increased number of type-V non-glandular trichomes  
363 compared to both MT and LA1777 (Fig 5B). It was shown earlier that there appears to be a negative  
364 correlation between densities of glandular type-IV trichomes and the non-glandular type-V trichomes  
365 (Vendemiatti *et al.*, 2017). The lower density of type-V trichomes in LA1777 could therefore be  
366 related to its high density of type-IV trichomes. The adult leaves of MT-*Sst2* and MT do not have  
367 type-IV glandular trichomes (Fig. 5B). This lack of type-IV trichomes in cultivated tomato has been  
368 linked to the transition from the juvenility to the adult phase (Vendemiatti *et al.*, 2017). So, the region

369 introgressed in MT-*Sst2* is most likely not involved in heterochrony and/or type-IV trichome  
370 development, though we cannot discard the possibility that the region introgressed harbors genes  
371 controlling the density of type-V trichomes, as we cannot explain the increased type-V density in the  
372 introgression line compared to MT.

373 **Genetic factors outside the *Sst2* metabolic cluster are required to produce sesquiterpene**  
374 **carboxylic acids (SCA) terpenoids and insect resistance**

375 Even though MT-*Sst2* produced relatively high levels of santalene and bergamotene,  
376 compared to *S. habrochaites* LA1777, this did not confer resistance to any of the herbivores tested  
377 here (Fig. 6). Herbivore resistance observed in the wild species is therefore likely due to the  
378 sesquiterpene carboxylic acids (SCAs) derivatives absent in MT-*Sst2*. We cannot rule out the  
379 contribution of type-IV trichomes-derived acylsugars in LA1777 (Kim *et al.*, 2012), but it has been  
380 shown before that the presence of SCAs in LA1777 modulates larval feeding behavior and survival  
381 of two tomato insect pests (Frelichowski and Juvik, 2001). On the other hand, transgenic *S.*  
382 *lycopersicum* producing the *S. habrochaites* sesquiterpene 7-epizingiberene, product of the  
383 expression of *zFPS* and *ShZIS*, probably an allelic variant of *ShSBS*, did display a clear toxicity  
384 phenotype against spider mites (Bleeker *et al.*, 2012). Transference of the complete SCA route to  
385 MT-*Sst2* will answer this question on the contribution of SCA in herbivore resistance.

386 Up to now, little is known about the enzymes catalyzing the formation of SCAs from  
387 sesquiterpenes in LA1777. It can be hypothesized that cytochrome P450 enzymes (which often  
388 hydroxylate terpenes) play a role. In *Santalum album* (Santalaceae) santalenes ( $\alpha$ -,  $\beta$ - and *epi*- $\beta$ -  
389 santalene) and  $\alpha$ -*exo*-bergamotene are further metabolized into sesquiterpene alcohols  $\alpha$ -,  $\beta$ -, and *epi*-  
390  $\beta$ -santalol and  $\alpha$ -*exo*-bergamotol by a CYP76F cytochrome P450 (Diaz-Chavez *et al.*, 2013).  
391 Nevertheless, co-expression of *S. album* santalene/bergamotene oxidase *SaCYP76F39v1* in  
392 transgenic tobacco plants did not hydroxylate santalene or bergamotene (Yin and Wong, 2019). In  
393 *Tanacetum cinerariifolium* (Asteraceae), two oxidation reactions convert trans-chrysanthemol into  
394 trans-chrysanthemic acid (H., Xu, Moghe, *et al.*, 2018). Using tomato transgenic lines, Xu *et al.*  
395 (2018a) also showed that expressing chrysanthemyl diphosphate synthase from *Tanacetum*  
396 *cinerariifolium* together with two an alcohol dehydrogenase and aldehyde dehydrogenase from the *S.*  
397 *habrochaites* LA1777 were sufficient for the transgenic fruits to produce trans-chrysanthemic acid.

398 Although the introgressed region in MT-*Sst2* contains both an alcohol dehydrogenase  
399 (ADH) and P450s from *S. habrochaites* LA1777, it seems that the genes required for the conversion  
400 of the terpenes to derivatization of the sesquiterpenes to their alcohols or carboxylic acids lie outside  
401 the metabolic cluster on chromosome 8. Peripheral pathway genes located outside the core metabolic

402 cluster in different chromosomes have been described before for tomato and other species (Nützmann  
403 *et al.*, 2016). The fact that we did not detect any sesquiterpene (intermediate) derivative in MT-*Sst2*  
404 indicates that the alcohol dehydrogenases and cytochrome P450s introgressed must have different  
405 functions.

406 Altogether, this study demonstrates that the plastid-derived sesquiterpene synthesis from *S.*  
407 *habrochaites* can be transferred to type-IV trichomes of cultivated tomato. However, additional  
408 genetic components from the wild species should be transferred to acquire herbivore resistance in  
409 cultivated tomato. The results presented here indicate that at least part of these genetic components  
410 is likely to encode: i) enzymes that convert santalene and bergamotene into their carboxylic acids, ii)  
411 transcription factors modulating the expression *zFPS* and *SBS* and iii) enzymes and possible  
412 regulatory genes for cell wall remodeling and enlargement of the internal cavity of the trichome gland.  
413 The introgressed line presented here, in the model system Micro-Tom, can provide for rapid  
414 introgression and transgenic manipulation of the additional genetic components involved in  
415 sesquiterpene metabolism and type-VI trichome morphology.

## 416 MATERIAL AND METHODS

### 417 Plant Material

418 Seeds from Micro-Tom (MT) were donated by Dr. Avram Levy (Weizmann Institute of  
419 Science, Israel) in 1998 and maintained through self-pollination as a true-to-type cultivar since then.  
420 The *lutescent 1* mutation was introgressed into MT from its original background as described  
421 previously in Carvalho *et al.* (2011). Seeds from *Solanum habrochaites* LA1777 were obtained from  
422 the Tomato Genetics Resource Center (TGRC - University of California).

423 The sesquiterpene synthase 2 pathway from *S. habrochaites* LA1777 was introgressed into  
424 MT background by allelic substitution making use of the morphological marker MT-*lutescent 1*,  
425 which maps on the same arm of chromosome 8 (<https://tgrc.ucdavis.edu/>) (Fig.1). Briefly, pollen  
426 from *S. habrochaites* LA1777 were collected and used to fertilize emasculated MT-*lutescent 1*  
427 flowers. The F1 obtained was used as pollen donor for MT-*lutescent 1* plants and this procedure was  
428 repeated in the successive backcrossing (BCs). In each BC, we screened for reduced plant size (MT-  
429 like phenotype) and the absence of the *lutescent 1* phenotype (Fig. S1), which is an indicative of the  
430 presence of the LA1777 genes in the *Sst2* locus. After self-pollination in BC<sub>6</sub>F<sub>2</sub> generation, we  
431 screened plants for the presence of the same sesquiterpenes compounds found in the wild parental  
432 species. The resulting homozygous MT-*Sst2* genotype was considered a near-isogenic line (NIL).

433 Plants were grown in a greenhouse with 30/26°C temperature day/night and 60–75% ambient  
434 relative humidity, 11.5 h/13 h (winter/summer) photoperiod, sunlight 250–350 µmol photons m<sup>-2</sup> s<sup>-1</sup>  
435 PAR irradiance. Seeds were germinated in bulk in 350 mL pots with a 1:1 mixture of commercial  
436 potting mix Basaplant® and expanded vermiculite, and was supplemented with 1 g L<sup>-1</sup> 10:10:10 NPK  
437 and 4 g L<sup>-1</sup> dolomite limestone (MgCO<sub>3</sub> + CaCO<sub>3</sub>). Upon the appearance of the first true leaf,  
438 seedlings of each genotype were individually transplanted to 150 mL pots containing the soil mix  
439 described above, except that NPK supplementation was increased to 8 g L<sup>-1</sup>.

440 **Genetic and Physical Mapping of the introgressed *Sst2* genes**

441 Genomic DNA isolation was extracted from leaflets using the method described by Fulton,  
442 Chunwongse & Tanksley (1995) with minor modifications. Molecular mapping using Cleaved  
443 Amplified Polymorphic Sequence (CAPS) markers was performed as previously described by  
444 Shavrukov (2016). Details of tomato genetic maps and chromosome 8 molecular markers can be  
445 accessed through the Solanaceous Genomics Network (<http://solgenomics.net/>). Primers and  
446 restriction enzymes yielding CAPS between tomato and *S. habrochaites* LA1777 are detailed in the  
447 Supplemental Table S1.

448 **Trichome counts and phenotyping**

449 Counting of trichomes density (mm<sup>2</sup>) were performed on leaflets taken from mature fifth  
450 leaves (counting from cotyledons) according to the methodology described by Vendemiatti *et al.*  
451 (2017). Both leaf surfaces were dissected along the longitudinal axis in 15 × 3 mm strips covering  
452 the middle section of the leaf blade (avoiding the primary veins). The strips were fixed on microscope  
453 slides using transparent nail polish. Five individuals per genotype were sampled, and four different  
454 strips were analyzed per plant. Images were taken using a Leica S8AP0 stereomicroscope (Wetzlar,  
455 Germany) magnifying glass set to 50x magnification, coupled to a Leica DFC295 camera (Wetzlar,  
456 Germany).

457 The morphology of type-VI trichomes was examined under an EVOSfl  
458 ([www.thermofisher.com](http://www.thermofisher.com)) inverted microscope. Lateral leaflets strips were submerged in water under  
459 microscope slides and images of type-VI trichomes were taken. All trichome measurements were  
460 performed on images of 5 plants per genotype using ImageJ software version 1.4.1. Gland volume  
461 and cavity volume were calculated using the volume of the prolate ellipsoid formula:  $V = 4/3 \times \pi \times$   
462  $a$  (vertical axis)  $\times b^2$  (horizontal axis).

463 **GC-MS quantification**

464 For GC-MS volatile terpene quantification 300 individual type-VI trichome glands were  
465 collected from leaves in adult vegetative phase (fifth leaf from the cotyledons) with a glass pulled  
466 Pasteur pipette under a Leica MZFLIII microscope ([www.leica-microsystems.com](http://www.leica-microsystems.com)). The terpene  
467 extraction was conducted according to the methodology described by Xu *et al.* (2018c). The collected  
468 glands were dissolved in 150 µL of hexane plus 0.5 ng µL of benzyl acetate (Sigma-Aldrich;  
469 [www.sigmaaldrich.com](http://www.sigmaaldrich.com)) as an internal standard. Na<sub>2</sub>CO<sub>3</sub> (Sigma-Aldrich) was used to remove water  
470 from the hexane. Volatiles were separated using an Agilent ([www.agilent.com](http://www.agilent.com)) 7890A gas  
471 chromatograph, attached to an Agilent 7200 accurate-mass quadrupole time-of-flight mass  
472 spectrometer. Here, 2µL of the sample was injected heated to 275°C in the injector port and separated  
473 on an HP-5ms column (0.25 mm in diameter, 30 m in length, with 0.25 µm film thickness) using  
474 Helium as carrier gas (flow rate 1 mL/min). The oven temperature was maintained at 40°C for 3 min  
475 and increased by 15°C per min until it reached 250°C and maintained for 3 min. Identification of the  
476 compounds was based on the retention time of the chromatographic peaks and their corresponding  
477 mass spectra, which were compared to terpene standards and data libraries. Quantification of peak  
478 areas was performed using Masshunter Qualitative Analysis software (Agilent). Peak areas were  
479 corrected for the internal standard and quantified using the available terpene standards. For  
480 compounds without terpene standards, we used the β-caryophyllene standard as a reference. Terpene  
481 concentration was calculated per trichome gland (ng/gland) using the peak areas relative to the  
482 internal (benzyl acetate) and terpene standards available.

#### 483 Whitefly bioassay

484 *Bemisia tabaci* (former biotype B; Middle East Asia Minor I-II (MEAM)) population was  
485 maintained in a climatized chamber (Snijders Tilburg; T 28°C, 16-h light, RH 75%) on cucumber  
486 plants prior to the experiment. For no-choice assay twenty adult whiteflies were randomly taken from  
487 the population, anesthetized with CO<sub>2</sub> and placed in a clipcage (2.5 cm diameter; Bioquip). Two  
488 clipcages were attached in two different leaflets per plant. Five plants per genotype were used. The  
489 plants were kept inside of a closed greenhouse compartment (28 °C, RH 65%) and after 5 days, the  
490 number of whiteflies alive was recorded.

#### 491 Spider Mite bioassay

492 A non-choice performance assay was set-up using two species of spider mites. The two  
493 spotted spider mite *T. urticae* Koch Viçosa-1 and the red spider mite *T. evansi* Baker & Pritchard  
494 Viçosa-1 were initially collected from infested tomato plants (Sarmento *et al.*, 2011). Before the  
495 experiments, *T. urticae* mites were maintained on detached leaves of *S. lycopersicum* cv. Santa Clara  
496 and *T. evansi* mites were maintained on detached leaves of *S. lycopersicum* cv. Castlemart following

497 standard procedures (Ataide *et al.*, 2016). The rearings were maintained in a climate room at 25 °C,  
498 a 16/8 h light regime with 300  $\mu\text{E m}^{-2} \text{s}^{-1}$ , and 60% RH.

499 For each plant genotype, 15 leaf discs of 15 mm were made from the fifth leaf (counting from  
500 the cotyledons). The leaf discs were placed on 1.5% daishin agar (Duchefa Biochemie bv, Haarlem,  
501 The Netherlands) that was poured in small cups (3 cm diameter x 2 cm height) with their adaxial side  
502 facing up. On each leaf disk, a single 2-day-old adult female of *T. urticae* or *T. evansi* was placed  
503 using a soft paintbrush. Mites were confined into each cup and ventilation was assured by a 1  $\text{cm}^2$   
504 opening on the lid that was covered with mite-proof mesh (pore size of 80  $\mu\text{m}$ ). The cups were  
505 maintained in a climate room at 25°C, a 16/8 h light regime with 300  $\mu\text{E m}^{-2} \text{s}^{-1}$ , and 60% RH. Two  
506 days after infestation, spider mite survival was recorded and the average fecundity (number of eggs  
507 laid per female) was calculated using those spider mites that were alive after the two-day period for  
508 the calculations.

509 **Thrips bioassay**

510 A non-choice performance thrips bioassay was set up using the western flower thrips  
511 *Frankliniella occidentalis* (Pergande). The thrips colony was kept in the laboratory inside cages  
512 where bean pods were provided and supplemented with pollen as previously described by Muñoz-  
513 Cárdenas et al., (2017). For each plant genotype, 15 leaf discs of 15 mm diameter were made. Similar  
514 to the spider mites set-up, the experimental arena consisted in cups (3 cm diameter x 2 cm height)  
515 filled with 1.5% Daishin agar on which one leaflet was placed with the adaxial side up. Five adult  
516 females were collected from the colony with the help of a 1 ml pipette tip attached to a vacuum and  
517 were released inside each cup through a small opening on the side of the cup, that was otherwise  
518 sealed with parafilm. The cups were maintained in a climate room at 25°C, a 16/8 h light regime with  
519 300  $\mu\text{E m}^{-2} \text{s}^{-1}$ , and 60% RH. 72 hours after the release of the females, the adult thrips were removed  
520 and their survival (number of alive thrips) was scored with the help of a dissecting stereoscope. The  
521 number of larvae that emerged from the eggs laid during the experiment was assessed 7 days after  
522 the beginning of the experiment.

523 **RNA Isolation and Quantitative RT-PCR**

524 Total RNA was extracted from trichomes isolated by shaking stems in liquid nitrogen with  
525 a vortex mixer. Total RNA was isolated using Trizol reagent (Invitrogen) according to the  
526 manufacturer's instructions. RNA treated with TURBO DNase (Ambion; [www.thermofisher.com](http://www.thermofisher.com))  
527 were reverse-transcribed to generate first-strand cDNA using RevertAid H Minus Reverse  
528 Transcriptase (Fermentas; [www.thermofisher.com](http://www.thermofisher.com)). cDNA was used as a template for quantitative  
529 RT-PCR (qRT-PCR). PCR reactions were performed using HOT FIREPol EvaGreen qPCR Mix Plus

530 (Solis Biodyne; [www.sbd.ee](http://www.sbd.ee)) and analyzed in an ABI 7500 Real-Time PCR System (Applied  
531 Biosystems; [www.appliedbiosystems.com](http://www.appliedbiosystems.com)). Two technical replicates were analyzed for at least three  
532 biological samples, together with template free reactions as negative controls. Transcript abundances  
533 were normalized to *Rubisco conjugating enzyme 1 (RCE1)* expression. Detailed primers information  
534 is described in the Supplemental Table S2.

535 **Experimental Design and Statistical Analysis**

536 Statistical analyses were done using SigmaPlot 11.0 for Windows. The experiments were  
537 arranged in a completely randomized design. All data were tested for normality and equal variance  
538 by Kolmogorov-Smirnov tests. The means were further analyzed by two-tailed Student's *t*-test ( $P \leq$   
539 0.05) or Fisher's LSD test ( $P \leq 0.05$ ) after one-way ANOVA in multiple comparisons. For data that do  
540 not assume a specified variance or normality, we performed ranking tests Wilcoxon rank sum for  
541 pairwise comparisons and Kruskal-Wallis one-way analysis for multiple groups.

542 **ACKNOWLEDGMENTS**

543 The authors thank L.E.P.P., P.B., R.S. and S.M.A.'s lab members for laboratory and  
544 greenhouse assistance.

545

546 **REFERENCES**

- 547 **Ataide, L.M.S., Pappas, M.L., Schimmel, B.C.J., Lopez-Orenes, A., Alba, J.M., Duarte,  
548 M.V.A., Pallini, A., Schuurink, R.C. and Kant, M.R.** (2016) Induced plant-defenses  
549 suppress herbivore reproduction but also constrain predation of their offspring. *Plant Sci.*, **252**,  
550 300–310.
- 551 **Balcke, G.U., Bennewitz, S., Bergau, N., Athmer, B., Henning, A., Majovsky, P., Jiménez-  
552 Gómez, J.M., Hoehenwarter, W. and Tissier, A.** (2017) Multi-Omics of tomato glandular  
553 trichomes reveals distinct features of central carbon metabolism supporting high productivity  
554 of specialized metabolites. *Plant Cell*, **29**, 960–983.
- 555 **Banerjee, A., Wu, Y., Banerjee, R., Li, Y., Yan, H. and Sharkey, T.D.** (2013) Feedback  
556 inhibition of deoxy-D-xylulose-5-phosphate synthase regulates the methylerythritol 4-  
557 phosphate pathway. *J. Biol. Chem.*, **288**, 16926–16936.
- 558 **Barry, C.S., Aldridge, G.M., Herzog, G., Ma, Q., McQuinn, R.P., Hirschberg, J. and  
559 Giovannoni, J.J.** (2012) Altered Chloroplast Development and Delayed Fruit Ripening  
560 Caused by Mutations in a Zinc Metalloprotease at the lutescent2 Locus of Tomato. *Plant  
561 Physiol.*, **159**, 1086–1098.
- 562 **Ben-Israel, I., Yu, G., Austin, M.B., et al.** (2009) Multiple biochemical and morphological factors  
563 underlie the production of methylketones in tomato trichomes. *Plant Physiol.*, **151**, 1952–  
564 1964.
- 565 **Bennewitz, S., Bergau, N. and Tissier, A.** (2018) QTL mapping of the shape of type VI glandular

- 566 trichomes in tomato. *Front. Plant Sci.*, **9**, 1421.
- 567 **Bergau, N., Bennewitz, S., Syrowatka, F., Hause, G. and Tissier, A.** (2015) The development of  
568 type VI glandular trichomes in the cultivated tomato *Solanum lycopersicum* and a related wild  
569 species *S. habrochaites*. *BMC Plant Biol.*, **15**, 289.
- 570 **Besser, K., Harper, A., Welsby, N., Schauvinhold, I., Slocombe, S., Li, Y., Dixon, R.A. and**  
571 **Broun, P.** (2009) Divergent regulation of terpenoid metabolism in the trichomes of wild and  
572 cultivated tomato species. *Plant Physiol.*, **149**, 499–514.
- 573 **Bleeker, P.M., Diergaarde, P.J., Ament, K., et al.** (2011) Tomato-produced 7-epizingiberene and  
574 R-curcumene act as repellents to whiteflies. *Phytochemistry*, **72**, 68–73.
- 575 **Bleeker, P.M., Mirabella, R., Diergaarde, P.J., et al.** (2012) Improved herbivore resistance in  
576 cultivated tomato with the sesquiterpene biosynthetic pathway from a wild relative. *Proc. Natl.*  
577 *Acad. Sci.*, **109**, 20124–20129.
- 578 **Bleeker, P.M., Spyropoulou, E.A., Diergaarde, P.J., et al.** (2011) RNA-seq discovery, functional  
579 characterization, and comparison of sesquiterpene synthases from *Solanum lycopersicum* and  
580 *Solanum habrochaites* trichomes. *Plant Mol. Biol.*, **75**, 323–336.
- 581 **Carvalho, R.F., Campos, M.L., Pino, L.E., Crestana, S.L., Zsögön, A., Lima, J.E., Benedito,**  
582 **V.A. and Peres, L.E.** (2011) Convergence of developmental mutants into a single tomato  
583 model system: “Micro-Tom” as an effective toolkit for plant development research. *Plant*  
584 *Methods*, **7**, 18.
- 585 **Coates, R.M., Denissen, J.F., Juvik, J.A. and Babka, B.A.** (1988) Identification of α-Santalenoic  
586 and Endo β-Bergamotenoic Acids as Moth Oviposition Stimulants from Wild Tomato Leaves.  
587 *J. Org. Chem.*, **53**, 2186–2192.
- 588 **Colby, S.M., Crock, J., Dowdle-Rizzo, B., Lemaux, P.G. and Croteau, R.** (1998) Germacrene C  
589 synthase from *Lycopersicon esculentum* cv. VFNT cherry tomato: cDNA isolation,  
590 characterization, and bacterial expression of the multiple product sesquiterpene cyclase. *Proc.*  
591 *Natl. Acad. Sci. U. S. A.*, **95**, 2216–21.
- 592 **Diaz-Chavez, M.L., Moniodis, J., Madilao, L.L., et al.** (2013) Biosynthesis of Sandalwood Oil:  
593 *Santalum album* CYP76F Cytochromes P450 Produce Santalols and Bergamotol. *PLoS One*, **8**,  
594 e75053.
- 595 **Dudareva, N., Andersson, S., Orlova, I., Gatto, N., Reichelt, M., Rhodes, D., Boland, W. and**  
596 **Gershenzon, J.** (2005) The nonmevalonate pathway supports both monoterpene and  
597 sesquiterpene formation in snapdragon flowers. *Proc. Natl. Acad. Sci. U. S. A.*, **102**, 933–938.
- 598 **Dudareva, N., Klempien, A., Muhlemann, J.K. and Kaplan, I.** (2013) Biosynthesis, function and  
599 metabolic engineering of plant volatile organic compounds. *New Phytol.*, **198**, 16–32.
- 600 **Eigenbrode, S.D., Trumble, J.T., Millar, J.G. and White, K.K.** (1994) Topical Toxicity of  
601 Tomato Sesquiterpenes to the Beet Armyworm and the Role of These Compounds in  
602 Resistance Derived from an Accession of *Lycopersicon hirsutum* f. typicum. *J. Agric. Food*  
603 *Chem.*, **42**, 807–810.
- 604 **Eigenbrode, S.D., Trumble, J.T. and White, K.K.** (1996) Trichome exudates and resistance to  
605 beet armyworm (Lepidoptera: Noctuidae) in *Lycopersicon hirsutum* f. typicum accessions.  
606 *Environ. Entomol.*, **25**, 90–95.
- 607 **Estévez, J.M., Cantero, A., Reindl, A., Reichler, S. and León, P.** (2001) 1-Deoxy-D-xylulose-5-

- 608 phosphate Synthase, a Limiting Enzyme for Plastidic Isoprenoid Biosynthesis in Plants. *J.  
609 Biol. Chem.*, **276**, 22901–22909.
- 610 **Falara, V., Akhtar, T.A., Nguyen, T.T.H., et al.** (2011) The tomato terpene synthase gene family.  
611 *Plant Physiol.*, **157**, 770–89.
- 612 **Frelichowski, J.E. and Juvik, J.A.** (2005) Inheritance of sesquiterpene carboxylic acid synthesis  
613 in crosses of *Lycopersicon hirsutum* with insect-susceptible tomatoes. *Plant Breed.*, **124**, 277–  
614 281.
- 615 **Frelichowski, J.E. and Juvik, J.A.** (2001) Sesquiterpene Carboxylic Acids from a Wild Tomato  
616 Species Affect Larval Feeding Behavior and Survival of *Helicoverpa zea* and *Spodoptera*  
617 *exigua* (Lepidoptera: Noctuidae). *J. Econ. Entomol.*, **94**, 1249–1259.
- 618 **Fulton, T.M., Chunwongse, J. and Tanksley, S.D.** (1995) Microprep protocol for extraction of  
619 DNA from tomato and other herbaceous plants. *Plant Mol. Biol. Report.*, **13**, 207–209.
- 620 **Glas, J.J., Schimmel, B.C.J., Alba, J.M., Escobar-Bravo, R., Schuurink, R.C. and Kant, M.R.**  
621 (2012) Plant glandular trichomes as targets for breeding or engineering of resistance to  
622 herbivores. *Int. J. Mol. Sci.*, **13**, 17077–17103.
- 623 **Gonzales-Vigil, E., Hufnagel, D.E., Kim, J., Last, R.L. and Barry, C.S.** (2012) Evolution of  
624 TPS20-related terpene synthases influences chemical diversity in the glandular trichomes of  
625 the wild tomato relative *Solanum habrochaites*. *Plant J. cell Mol. Biol.*, **71**, 921–935.
- 626 **Hoeven van der, R.S., Monforte, A.J., Breeden, D., Tanksley, S.D. and Steffens, J.C.** (2000)  
627 Genetic control and evolution of sesquiterpene biosynthesis in *Lycopersicon esculentum* and  
628 *L. hirsutum*. *Plant Cell*, **12**, 2283–2294.
- 629 **Kang, J.-H., Shi, F., Jones, A.D., Marks, M.D. and Howe, G.A.** (2010) Distortion of trichome  
630 morphology by the hairless mutation of tomato affects leaf surface chemistry. *J. Exp. Bot.*, **61**,  
631 1053–1064.
- 632 **Kang, J.H., Gonzales-Vigil, E., Matsuba, Y., Pichersky, E. and Barry, C.S.** (2014)  
633 Determination of residues responsible for substrate and product specificity of *Solanum*  
634 *habrochaites* short-chain cis-prenyltransferases. *Plant Physiol.*, **164**, 80–91.
- 635 **Kim, J., Kang, K., Gonzales-Vigil, E., Shi, F., Jones, A.D., Barry, C.S. and Last, R.L.** (2012)  
636 Striking natural diversity in glandular trichome acylsugar composition is shaped by variation at  
637 the Acyltransferase2 locus in the wild tomato *Solanum habrochaites*. *Plant Physiol.*, **160**,  
638 1854–70.
- 639 **Maluf, W.R., Campos, G.A. and Graças Cardoso, M. Das** (2001) Relationships between  
640 trichome types and spider mite (*Tetranychus evansi*) repellence in tomatoes with respect to  
641 foliar zingiberene contents. *Euphytica*, **121**, 73–80.
- 642 **Matsuba, Y., Nguyen, T.T.H., Wiegert, K., et al.** (2013) Evolution of a complex locus for terpene  
643 biosynthesis in *Solanum*. *Plant Cell*, **25**, 2022–2036.
- 644 **Moodley, V., Gubba, A. and Mafongoya, P.L.** (2019) A survey of whitefly-transmitted viruses on  
645 tomato crops in South Africa. *Crop Prot.*, **123**, 21–29.
- 646 **Muñoz-Cárdenas, K., Ersin, F., Pijnakker, J., et al.** (2017) Supplying high-quality alternative  
647 prey in the litter increases control of an above-ground plant pest by a generalist predator. *Biol.  
648 Control*, **105**, 19–26.

- 649 Nützmann, H.W., Huang, A. and Osbourn, A. (2016) Plant metabolic clusters – from genetics to  
650 genomics. *New Phytol.*, **211**, 771–789.
- 651 Sallaud, W.C., Rontein, D., Onillon, S., et al. (2009) A Novel Pathway for Sesquiterpene  
652 Biosynthesis from Z,Z-Farnesyl Pyrophosphate in the Wild Tomato Solanum habrochaites.  
653 *Plant Cell*, **21**, 301–317.
- 654 Sarmento, R.A., Lemos, F., Bleeker, P.M., et al. (2011) A herbivore that manipulates plant  
655 defence. *Ecol. Lett.*, **14**, 229–236.
- 656 Schilmiller, A.L., Schauvinhold, I., Larson, M., Xu, R., Charbonneau, A.L., Schmidt, A.,  
657 Wilkerson, C., Last, R.L. and Pichersky, E. (2009) Monoterpenes in the glandular trichomes  
658 of tomato are synthesized from a neryl diphosphate precursor rather than geranyl diphosphate.  
659 *Proc. Natl. Acad. Sci. U. S. A.*, **106**, 10865–10870.
- 660 Shavrukov, Y.N. (2016) CAPS markers in plant biology. *Russ. J. Genet. Appl. Res.*, **6**, 279–287.
- 661 Silva, G.A., Picanço, M.C., Bacci, L., Crespo, A.L.B., Rosado, J.F. and Guedes, R.N.C. (2011)  
662 Control failure likelihood and spatial dependence of insecticide resistance in the tomato  
663 pinworm, *Tuta absoluta*. *Pest Manag. Sci.*, **67**, 913–920.
- 664 Simmons, A.T. and Gurr, G.M. (2005) Trichomes of *Lycopersicon* species and their hybrids:  
665 Effects on pests and natural enemies. *Agric. For. Entomol.*, **7**, 265–276.
- 666 Spyropoulou, E.A., Haring, M.A. and Schuurink, R.C. (2014) RNA sequencing on *Solanum*  
667 *lycopersicum* trichomes identifies transcription factors that activate terpene synthase  
668 promoters. *BMC Genomics*, **15**, 1–16.
- 669 Tanksley, S.D., Ganal, M.W., Prince, J.P., et al. (1992) High density molecular linkage maps of  
670 the tomato and potato genomes. *Genetics*, **132**, 1141–1160.
- 671 Tholl, D. (2006) Terpene synthases and the regulation, diversity and biological roles of terpene  
672 metabolism. *Curr. Opin. Plant Biol.*, **9**, 297–304.
- 673 Tissier, A. (2012) Glandular trichomes: what comes after expressed sequence tags?. *Plant J.*, **70**,  
674 51–68.
- 675 Van Schie CCN, Haring MA, Schuurink RC (2007) Tomato linalool synthase is induced in  
676 trichomes by jasmonic acid. *Plant Mol Biol* **64**: 251–63
- 677 Vendemiatti, E., Zsögön, A., Silva, G.F.F. e, Jesus, F.A. de, Cutri, L., Figueiredo, C.R.F.,  
678 Tanaka, F.A.O., Nogueira, F.T.S. and Peres, L.E.P. (2017) Loss of type-IV glandular  
679 trichomes is a heterochronic trait in tomato and can be reverted by promoting juvenility. *Plant*  
680 *Sci.*, **259**, 35–47.
- 681 Wakil, W., Brust, G.E. and Perring, T.M. (2018) Tomato and Management of Associated  
682 Arthropod Pests: Past, Present, and Future. In *Sustainable Management of Arthropod Pests of*  
683 *Tomato*. pp. 3–12.
- 684 Xu, H., Lybrand, D., Bennewitz, S., Tissier, A., Last, R.L. and Pichersky, E. (2018) Production  
685 of trans-chrysanthemic acid, the monoterpane acid moiety of natural pyrethrin insecticides, in  
686 tomato fruit. *Metab. Eng.*, **47**, 271–278.
- 687 Xu, H., Moghe, G.D., Wiegert-Rininger, K., Schilmiller, A.L., Barry, C.S., Last, R.L. and  
688 Pichersky, E. (2018) Coexpression Analysis Identifies Two Oxidoreductases Involved in the  
689 Biosynthesis of the Monoterpane Acid Moiety of Natural Pyrethrin Insecticides in Tanacetum

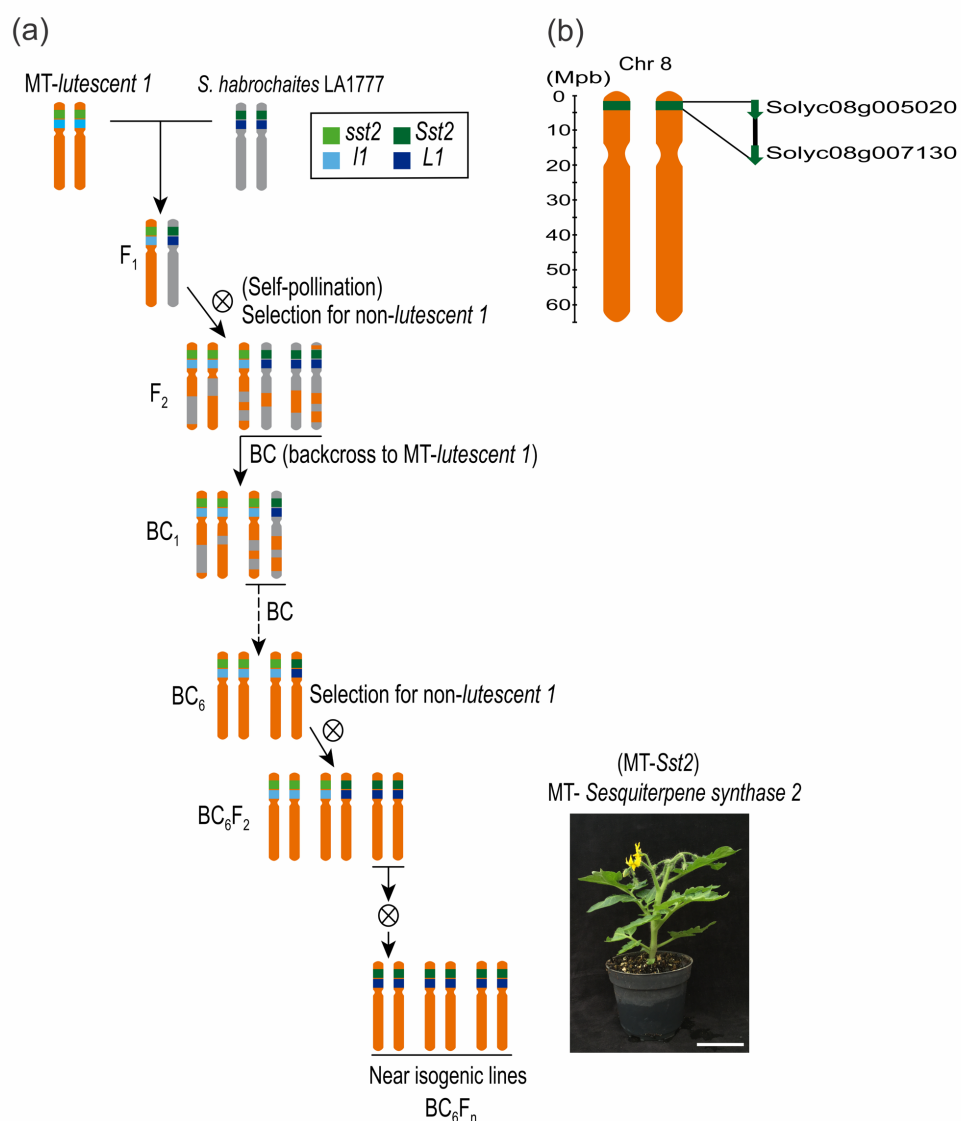
690 *cinerariifolium*. *Plant Physiol.*, **176**, 524–537.

691 Xu, J., Herwijnen, Z.O. van, Dräger, D.B., Sui, C., Haring, M.A. and Schuurink, R.C. (2018)  
692 SlMYC1 Regulates type VI glandular trichome formation and terpene biosynthesis in tomato  
693 glandular cells. *Plant Cell*, **30**, 2988–3005.

694 **Yin, J.L. and Wong, W.S. (2019) Production of santalenes and bergamotene in Nicotiana tabacum**  
695 **plants. *PLoS One*, 14, e0203249.**

696

697 FIGURES



698

699

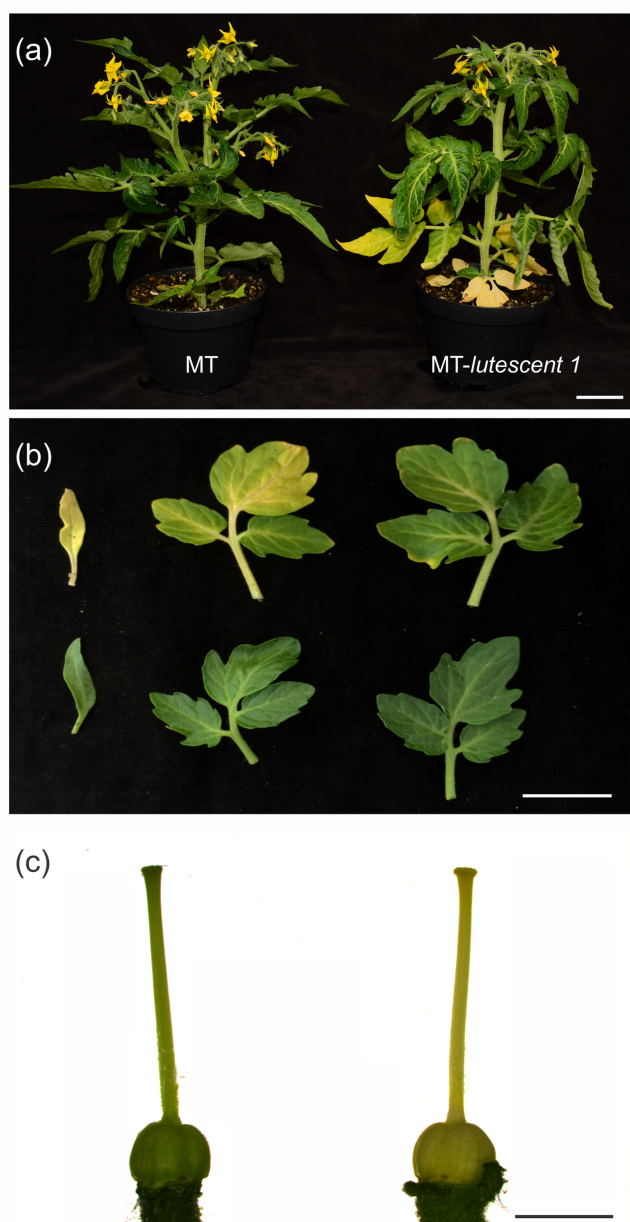
**Fig. 1** Scheme of crossing and backcrossing (BC) to create a Micro-Tom (MT) near isogenic line (NIL) harboring the *Solanum habrochaites* LA1777 genes for the “Sesquiterpene Synthase 2” (*SsT2*) locus. **(a)** MT NIL bearing the *lutescent 1* mutation was used to assist the introgression process as a morphological marker (the absence of the *lutescent 1* phenotype was used as an indicator of the presence of the LA1777 genes in the *SsT2* locus). The presence of MT (*l1* and *sst2*) or LA1777 (*L1* and *Sst2*) variants is indicated in different colors. **(b)** The ID (Solyc) of the genetic markers used to determine the introgression borders are depicted.

707

708

709

710



711

712

713

714

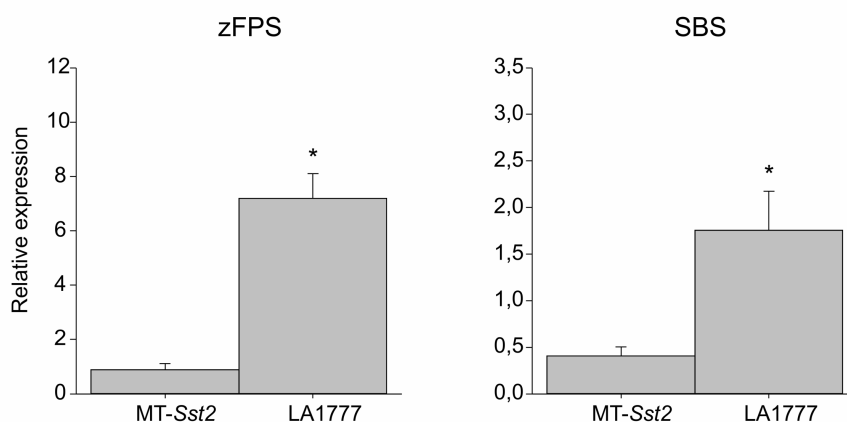
715

716

717

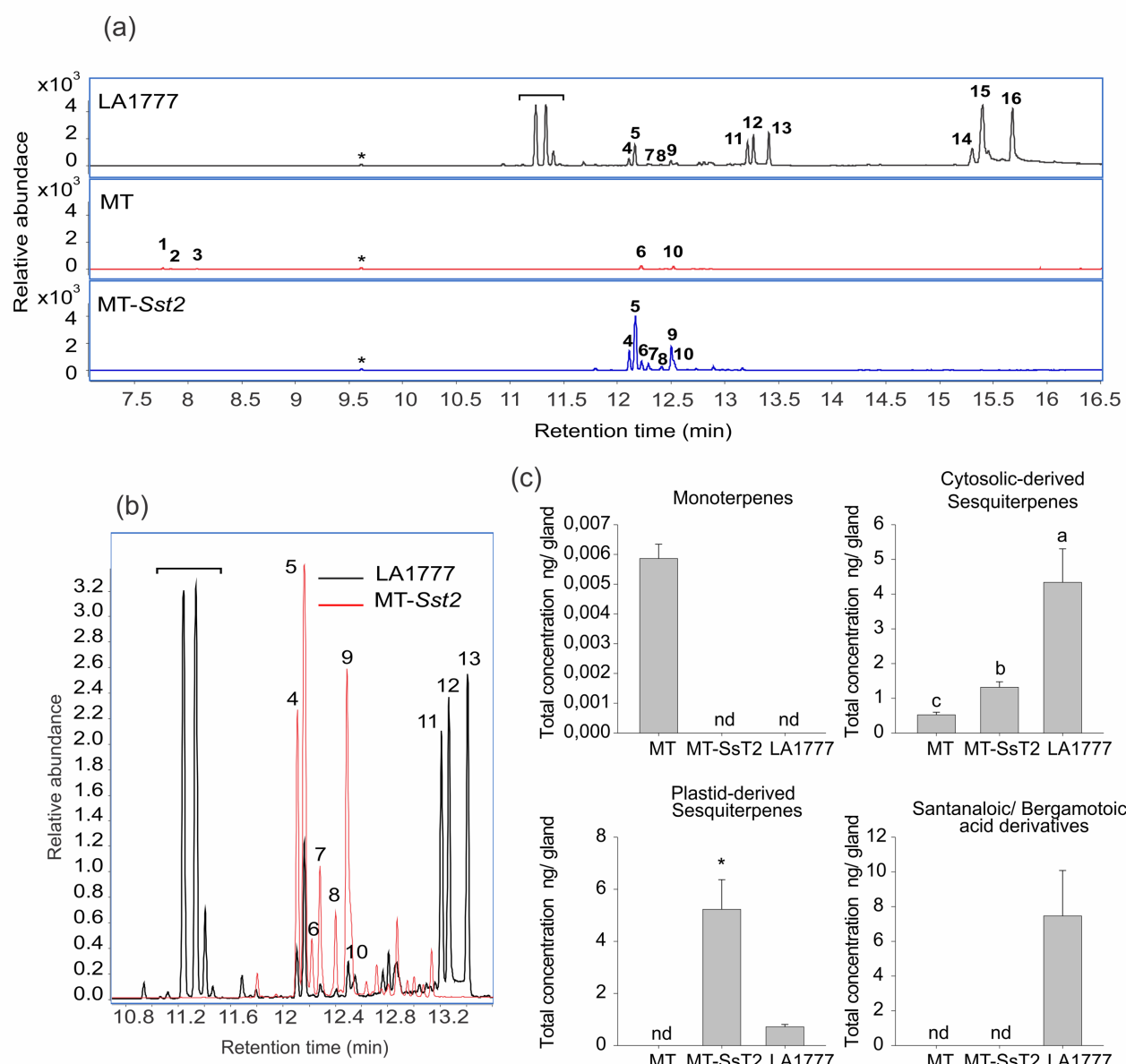
718

**Fig. S1 (a)** Representative MT and the MT near isogenic line (NIL) harboring the *lutescent 1* (l/l) mutation (MT-*lutescent 1*) which shows a premature and progressive chlorophyll loss that was used as a morphological marker for genetic introgression. Bar = 2 cm. **(b)** MT-*lutescent 1* leaf phenotype (top) displaying premature and progressive chlorophyll loss on cotyledons and the first and second leaves, compared with MT (bottom), which do not present senescent-like leaves at this developmental stage. Bar = 3 cm. **(c)** MT-*lutescent 1* pistil (right) with chlorophyll loss, compared with MT pistil (left). Bar = 2 mm. The photos were taken from 45-days old plants.



719

720 **Fig. 2.** Transcript levels of the *SsT2* locus-derived genes *cis*-Farnesyl Diphosphate Synthase (*zFPS*) and  
721 *Santalene and Bergamotene Synthase* (*SBS*) in trichomes from MT-*Sst2* and *S. habrochaites* LA1777. Mean  
722 values of 4 biological replicates are shown. Transcript levels were normalized for *Rubisco conjugating*  
723 *enzyme 1* (RCE1). Asterisks indicate mean significantly different from MT-*Sst2*, according to Student t-test  
724 ( $P \leq 0,05$ ).



725

726

727

728

729

730

731

732

733

734

735

736

737

738

739

740

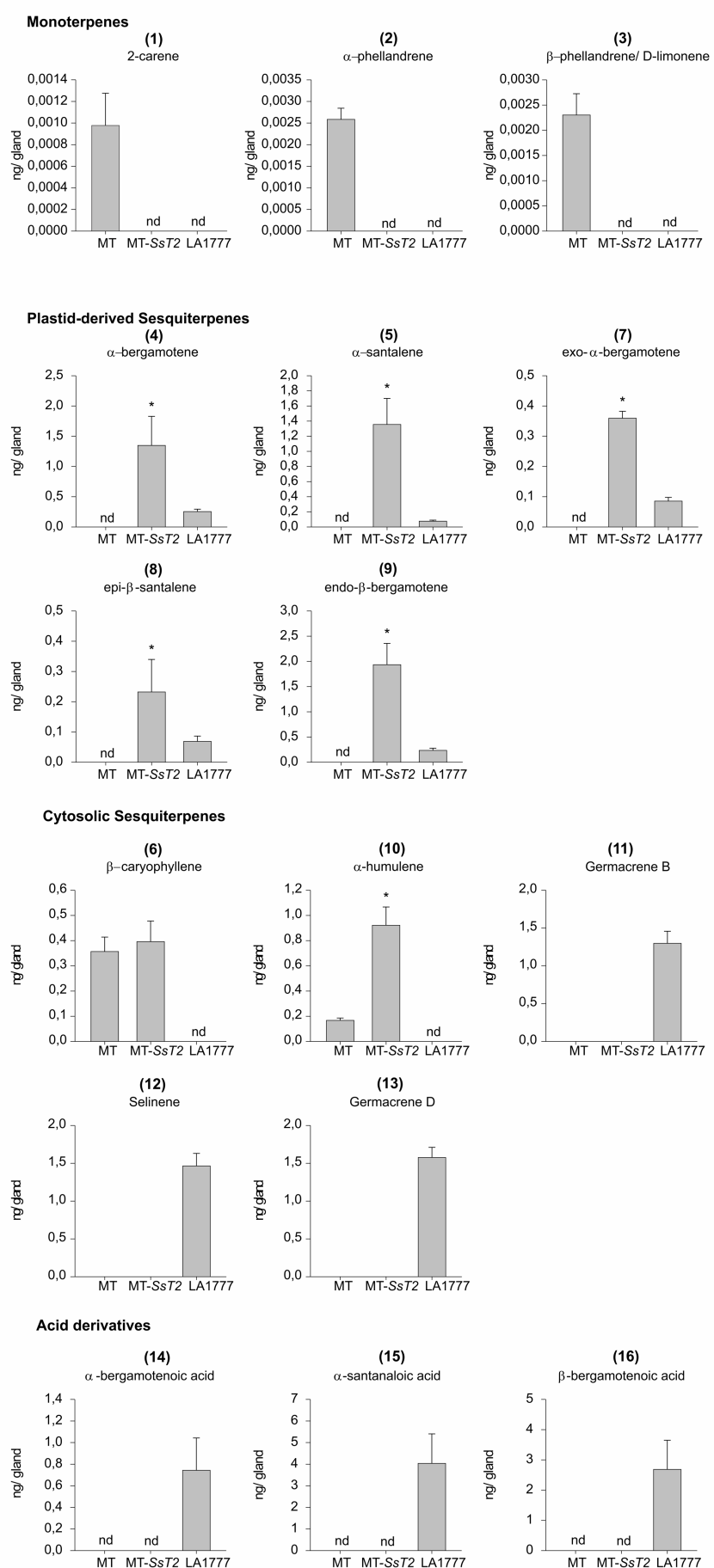
741

742

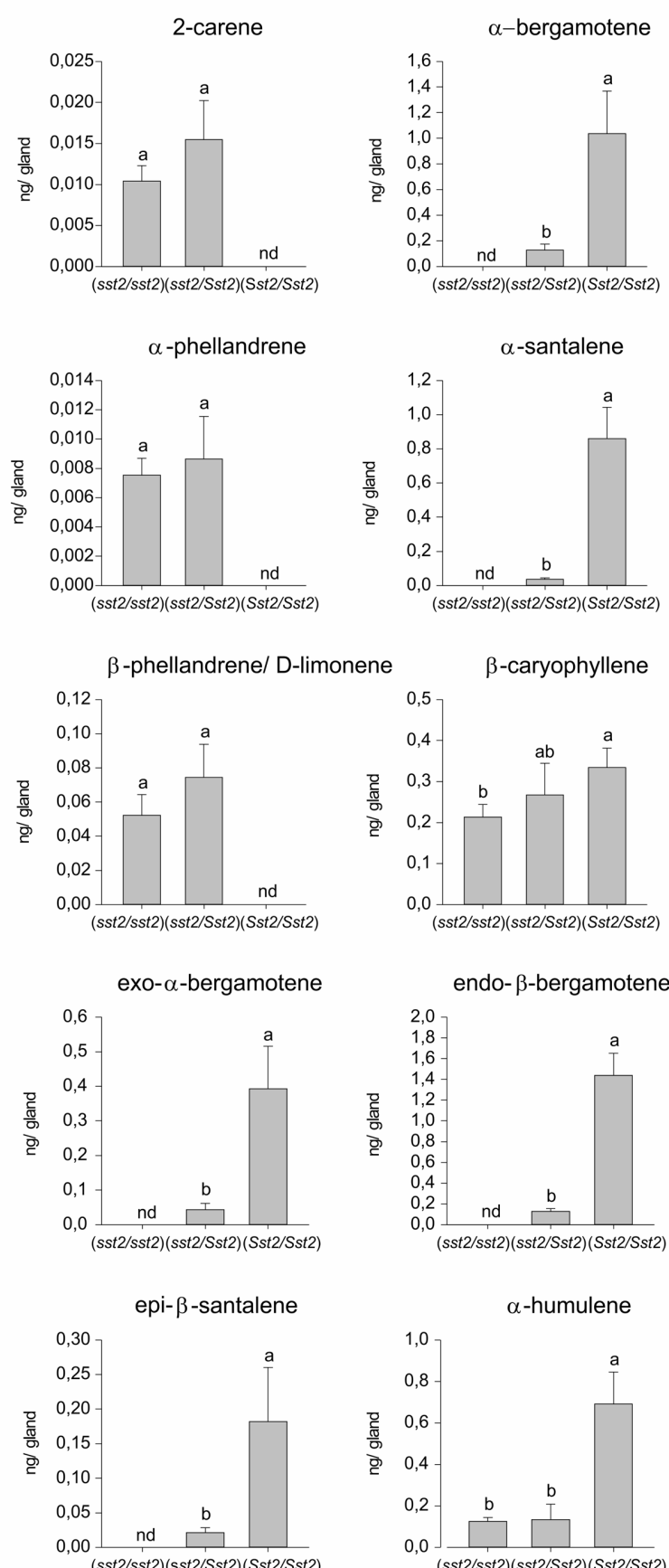
743

**Fig. 3 (a)** GC-MS chromatograms showing mono and sesquiterpenes found in type-VI trichomes from Micro-Tom (MT), MT-Sst2, and *S. habrochaites* LA1777. The indicated peaks corresponds to the following compounds: (1) 2-carene, (2)  $\alpha$ -phellandrene, (3)  $\beta$ -phellandrene/ D-limonene, (4)  $\alpha$ -bergamotene, (5)  $\alpha$ -santalene, (6)  $\beta$ -caryophyllene, (7) exo- $\alpha$ -bergamotene, (8) epi- $\beta$ -santalene, (9) endo- $\beta$ -bergamotene, (10)  $\alpha$ -humulene, (11) germacrene B, (12) selinene, (13) germacrene D, (14)  $\alpha$ -bergamotic acid, (15)  $\alpha$ -santalanoic acid and (16)  $\beta$ -bergamotic acid. The asterisks indicate the peaks related to the internal standard. The bracket indicates peaks related to unidentified putatively lipid-originating compounds. The chromatogram shows the detector response for the ion mass 93.069 and 108.056. **(b)** Gas chromatograms overlaying sesquiterpenes found in type-VI trichomes from MT-Sst2 and *Solanum habrochaites* LA1777. The bracket indicates peaks related to unidentified putatively lipid-originating compounds. **(c)** Total amount of compounds present in type-VI glandular trichomes of each genotype. Total concentration of monoterpenes: (1) 2-carene, (2)  $\alpha$ -phellandrene and (3)  $\beta$ -phellandrene/ D-limonene; Total concentration of cytosolic sesquiterpenes: (6)  $\beta$ -caryophyllene, (10)  $\alpha$ -humulene, (11) germacrene B, (12) selinene and (13) germacrene D; Total concentration of plastid-derived sesquiterpenes: (4)  $\alpha$ -bergamotene, (5)  $\alpha$ -santalene, (7) exo- $\alpha$ -bergamotene, (8) epi- $\beta$ -santalene and (9) endo- $\beta$ -bergamotene; Total concentration of santalanoic/ bergamotic acid derivative: (14)  $\alpha$ -bergamotic acid, (15)  $\alpha$ -santalanoic acid (16)  $\beta$ -bergamotic acid. The bars represent the mean  $\pm$  SE of five biological replicates. For each sample, 300 type-VI glandular trichomes were collected with a glass capillary for GC-MS analysis. Bars indicated with an asterisk were significantly different according to t-test ( $P \leq 0.05$ ).

744 Bars indicated with different letters were significantly different according to Fisher's LSD test ( $P \leq 0.05$ )  
745 after ANOVA. nd, Not detected.  
746



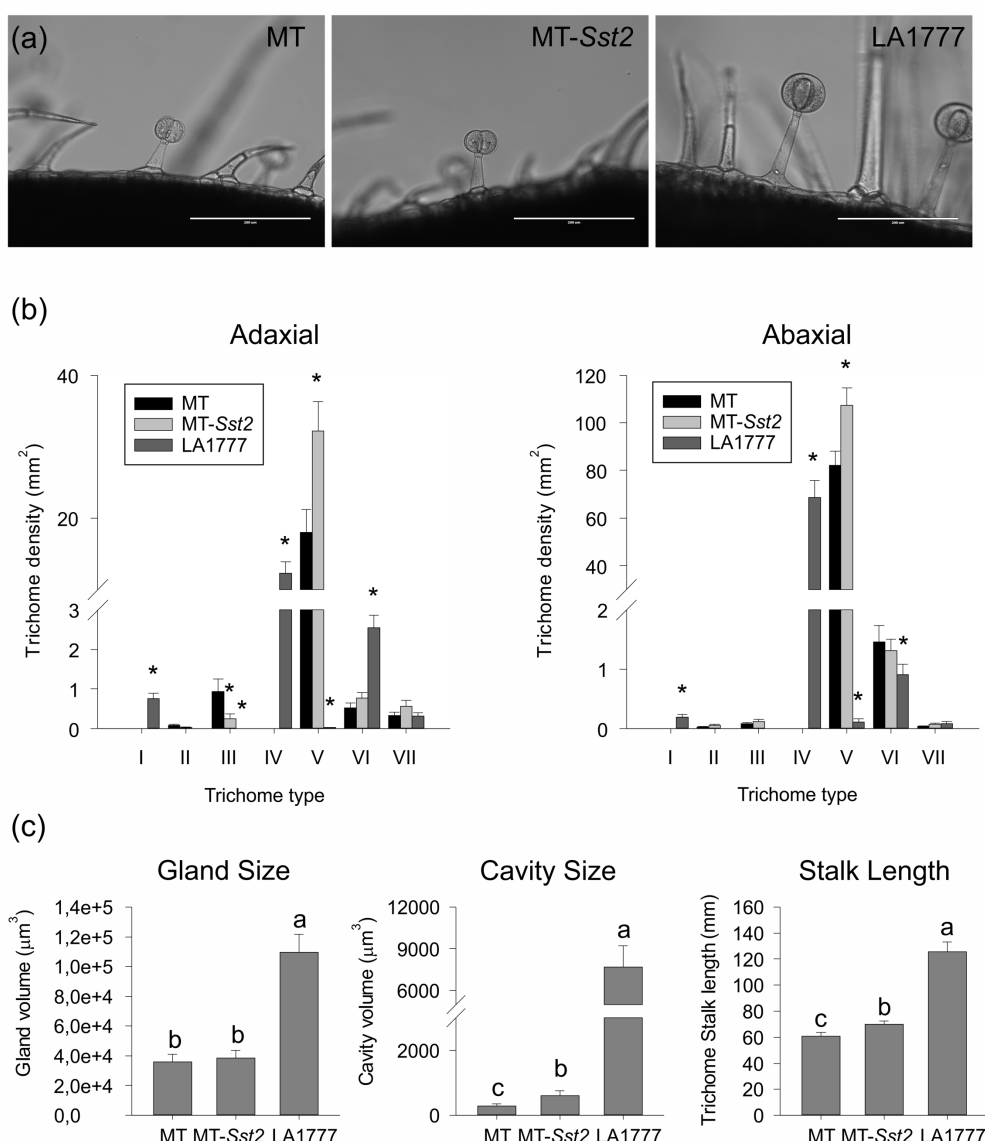
748      **Fig. S2.** Volatile terpene levels in type-VI glandular trichomes from Micro-Tom (MT), MT-*Sst2* and the wild  
749      species *Solanum habrochaites* LA1777. The data show the amount of each compounds present in type-VI  
750      glandular trichomes. Each data point represents the mean + SE of five biological replicates. For each sample,  
751      300 type-VI glandular trichomes were collected with a glass capillary before GC-MS. Means indicated with  
752      an asterisk were significantly different according to t-test ( $P \leq 0.05$ ). nd, Not detected.  
753  
754



755  
756  
757  
758  
759

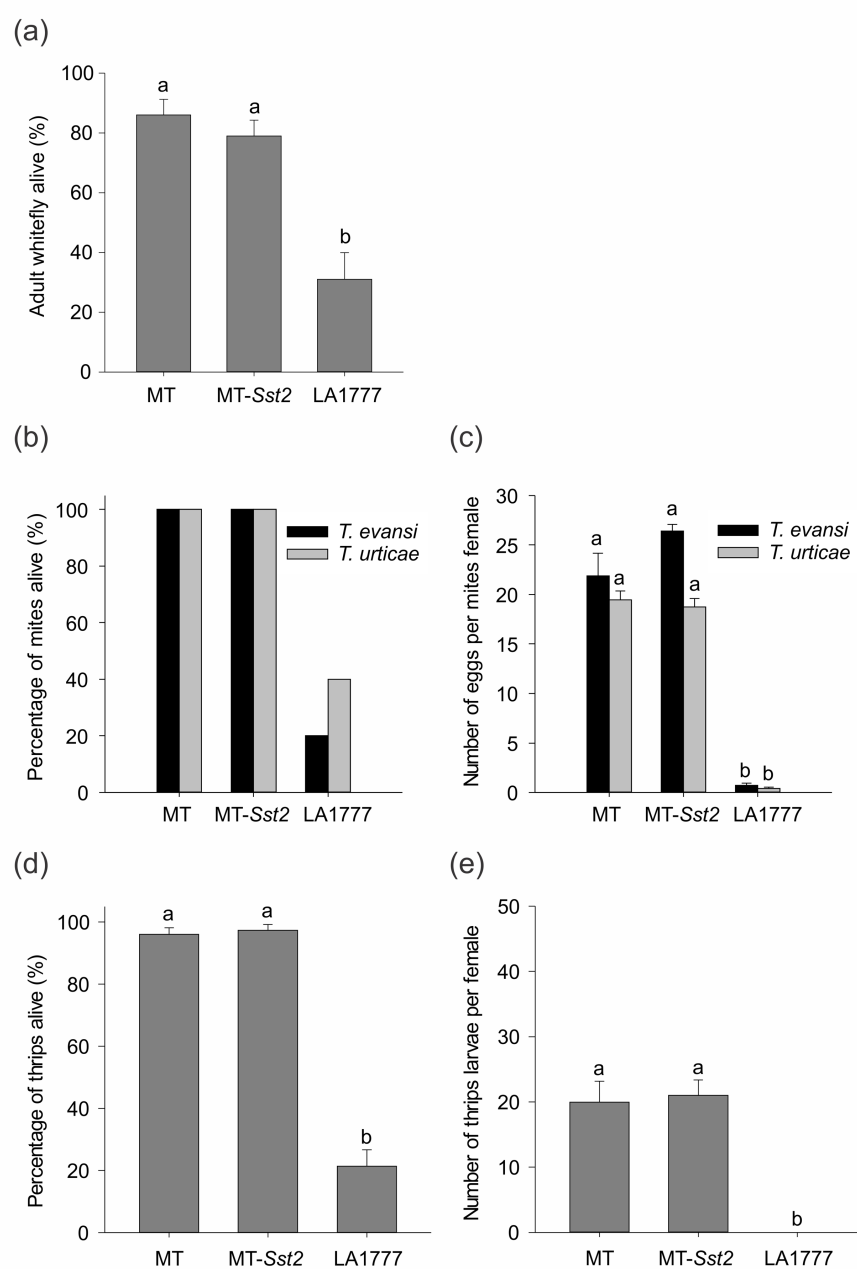
**Fig. 4** Volatile terpene levels in type-VI glandular trichomes from Micro-Tom plants homozygous (*sst2/sst2*, *Sst2/Sst2*) and hemizygous (*sst2/Sst2*) at the *Sst2* locus. The data show the amount of each compound present in type-VI glandular trichomes. Each data point represents the mean and SE of five biological replicates. For each sample, 300 type-VI glandular trichomes were collected with a glass capillary before

760 GC-MS. Bars indicated with different letters were significantly different according to Fisher's LSD test ( $P \leq$   
761 0.05) after ANOVA. nd, Not detected.  
762



763

764 **Fig. 5. (a)** Bright field microscopy of trichomes on the leaf surface of representative 45-days old plants of  
765 Micro-Tom (MT), MT-Sst2, and *Solanum habrochaites* LA1777. Scale bar = 200  $\mu\text{m}$ . **(b)** Density ( $\text{mm}^{-2}$ ) of  
766 trichome types on adaxial and abaxial leaf surfaces. Data are mean ( $n=40$ ) for each surface. Asterisks indicate  
767 mean significantly different from the control MT, according to Student t-test ( $P \leq 0.05$ ). **(c)** Trichome gland  
768 size, cavity volume and stalk length of type-VI trichomes. Data are mean ( $\pm \text{SE}$ ) of 20 trichomes of 2 replicate  
769 leaves of five plants. Bars indicated with different letters were significantly different according to Fisher's  
770 LSD test ( $P \leq 0.05$ ) after ANOVA.



771

772 **Fig. 6.** Herbivory tests performed on Micro-Tom (MT), MT-Sst2 and *Solanum habrochaites* LA1777  
773 genotypes. (a) Percentage of adult whitefly *Bemisia tabaci* alive after five days of feeding on leaves. Data  
774 are means ( $\pm$ SE) of five plants, each with two cages. Bars indicated with different letters were significantly  
775 different according to Fisher's LSD test ( $P \leq 0.05$ ) after ANOVA. (b) and (c) Female spider mite  
776 (*Tetranychus evansi* and *Tetranychus urticae*) survival and number of eggs after two days of feeding on  
777 plants. Bars indicated with different letters were significantly different according to Fisher's LSD test ( $P \leq$   
778 0.05) after ANOVA. (d) and (e) Percentage of adult thrips alive and number of thrips larvae per female that  
779 emerged after two days on leaf discs. Bars indicated with different letters were significantly different  
780 according to Fisher's LSD test ( $P \leq 0.05$ ) after ANOVA.

781

782

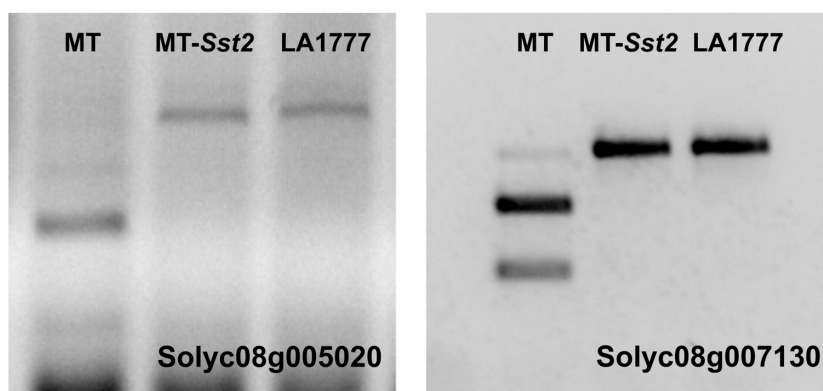
783

784 **Table S1.** Oligonucleotide sequence used for CAPS markers.

Locus id <sup>1</sup>	Forward	Reverse	Enzyme	MT	LA1777
Solyc08g005020	TTTGC GTGTACCTTT GCAG	TCCTCCTCAAAACCC TCTTCCTC	HinfI	536/512/ 239	1048/ 239
Solyc08g005640	GTTCTCATAGTTCCA CTATGTATCC	GACAAACTACTTTGT TGTCGGAGT	HindIII	693/155/ 322	693/477
Solyc08g006410	GATCCATTCCTTCCTT GGGCTGTTG	GATGGTATTGTTGGT CCAATTGTC	PacI	605	503/102
Solyc08g007130	GTCCTTGTTGGTGAAC AAGATATCC	GAATATGCCCTCTGC TGATGCTAGG	BglII	986/490	1478
Solyc08g065740	CGGTGGTCTTAAGGAT GAGAAC	CACAAC TCAAAATA GGGTCTC	BanI	81/286/ 342	367/342
Solyc08g076820	GTACTACTACTCCCTT AGAGCAAC	GTATGC ACTAGGGCT CATAATT CG	BspDI	536/125	661
Solyc08g083230	GATGTGGGTTGTTTG CAGGA	CCAGACATGGAAAGT GTTAGCGA	TaqI	618/179/ 106	797/106

785 Locus according to Sol Genomics Network database (<http://solgenomics.net/>).

786



787

788 **Fig. S3** Electrophoresis gels showing the positive genetic markers used to differentiate MT-Sst2  
789 from MT.

790

791 **Table S2.** Oligonucleotide sequence used for quantitative PCR analyses.

Primer name	Sequence	Gene symbol	References
SBS_QF	GCATTACAGAATGAGTCGAGG	LOC101250138	-

---

SBS_QR	CTGATGGTAAATCAAGGCAGC		
ZFPS_QF	TTTCGAGGTCTGGAGTAAGAGTG	AHF95235	-
ZFPS_QR	TAGTGCAATCACAAAGGTGAAGTC		
RCE1_QF	GATTCTCTCTCATCAATCAATTG	TC153679	(Van Schie et al., 2007)
RCE1_QR	GAACGTAAATGTGCCACCCATA		

---

792 Gene symbol according to National Center for Biotechnology Information database  
793 (<https://www.ncbi.nlm.nih.gov/>).

794

795

796